

Fluorescence, XPS, and TOF-SIMS Surface Chemical State Image Analysis of DNA Microarrays

Chi-Ying Lee,^{†,§} Gregory M. Harbers,^{||,⊥} David W. Grainger,^{||,⊥} Lara J. Gamble,^{†,‡} and David G. Castner^{*,†,‡,§}

Contribution from the National ESCA and Surface Analysis Center for Biomedical Problems, Departments of Bioengineering and Chemical Engineering, Box 351750, University of Washington, Seattle, Washington 98195-1750, and Departments of Pharmaceutics and Pharmaceutical Chemistry, and Bioengineering, University of Utah, Salt Lake City, Utah 84112-5820

Received March 16, 2007; E-mail: castner@nb.engr.washington.edu

Abstract: Performance improvements in DNA-modified surfaces required for microarray and biosensor applications rely on improved capabilities to accurately characterize the chemistry and structure of immobilized DNA molecules on micropatterned surfaces. Recent innovations in imaging X-ray photoelectron spectroscopy (XPS) and time-of-flight secondary ion mass spectrometry (TOF-SIMS) now permit more detailed studies of micropatterned surfaces. We have exploited the complementary information provided by imaging XPS and imaging TOF-SIMS to detail the chemical composition, spatial distribution, and hybridization efficiency of amine-terminated single-stranded DNA (ssDNA) bound to commercial polyacrylamide-based, amine-reactive microarray slides, immobilized in both macrospot and microarray diagnostic formats. Combinations of XPS imaging and small spot analysis were used to identify micropatterned DNA spots within printed DNA arrays on slide surfaces and quantify DNA elements within individual microarray spots for determination of probe immobilization and hybridization efficiencies. This represents the first report of imaging XPS of DNA immobilization and hybridization efficiencies for arrays fabricated on commercial microarray slides. Imaging TOF-SIMS provided distinct analytical data on the lateral distribution of DNA within single array microspots before and after target hybridization. Principal component analysis (PCA) applied to TOF-SIMS imaging datasets demonstrated that the combination of these two techniques provides information not readily observable in TOF-SIMS images alone, particularly in identifying species associated with array spot nonuniformities (e.g., “halo” or “donut” effects often observed in fluorescence images). Chemically specific spot images were compared to conventional fluorescence scanned images in microarrays to provide new information on spot-to-spot DNA variations that affect current diagnostic reliability, assay variance, and sensitivity.

Introduction

Patterning DNA onto surfaces has recently received considerable attention due to its applications in fundamental biology and biomedical research as genomic arrays, diagnostics, and biosensors.^{1,2} Several methods have been developed for fabricating micron-scale DNA patterns, including contact and noncontact printing of presynthesized DNA onto substrates, and in situ synthesis of microarrays using electrochemistry³ and photolithography.^{4–6} Microprinting techniques are widely used for DNA

microarray fabrication on commercial array slides containing hundreds to thousands of spotted features. The printing process generally involves spatially controlled delivery of nanoliter drops of DNA solutions onto reactively coated glass substrates using a robotic spotter, followed by evaporation of deposited liquid droplets within seconds. This rapid evaporative process produces increased solution ionic strength and solute concentrations in the drying DNA film, resulting in distinct differences in immobilized DNA structure, density, and chemistry compared to bulk solution coupling reactions between DNA and surfaces.^{5,7} A common observation is the formation of dry DNA spots with greater DNA density at the edges than in the middle as solution flows to the spot edge upon rapid evaporation.⁸ In addition, surface damage may also occur during the array printing process, especially with contact-based printing meth-

[†] National ESCA and Surface Analysis Center for Biomedical Problems, University of Washington.

[‡] Department of Bioengineering, University of Washington.

[§] Department of Chemical Engineering, University of Washington.

^{||} Department of Pharmaceutics and Pharmaceutical Chemistry, University of Utah.

[⊥] Department of Bioengineering, University of Utah.

(1) Bejjani, B. A.; Shaffer, L. G. *J. Mol. Diagn.* **2006**, *8*, 528–533.

(2) Lamartine, J. *Mater. Sci., Eng. C* **2006**, *26*, 354–359.

(3) Egeland, R. D.; Southern, E. M. *Nucleic Acids Res.* **2005**, *33*, e125.

(4) Barbulovic-Nad, I.; Lucente, M.; Sun, Y.; Zhang, M. J.; Wheeler, A. R.; Bussmann, M. *Crit. Rev. Biotechnol.* **2006**, *26*, 237–259.

(5) Dufva, M. *Biomol. Eng.* **2005**, *22*, 173–184.

(6) Pirrung, M. C. *Angew. Chem., Int. Ed.* **2002**, *41*, 1276–1289.

(7) Gong, P.; Harbers, G. M.; Grainger, D. W. *Anal. Chem.* **2006**, *78*, 2342–2351.

(8) Ramakrishnan, R.; Dorris, D.; Lublinsky, A.; Nguyen, A.; Domanus, M.; Prokhorova, A.; Gieser, L.; Touma, E.; Lockner, R.; Tata, M.; Zhu, X. M.; Patterson, M.; Shippy, R.; Sendera, T. J.; Mazumder, A. *Nucleic Acids Res.* **2002**, *30*, e30.

ods.⁶ The resulting immobilized DNA density and distribution within individual microarray spots have profound influences on the subsequent target capture performance.^{9,10} Spot-to-spot variations in DNA surface density and distribution can therefore lead to inconsistent target capture, inaccurate data quantification, and misleading results. Thus, accurate quantitative analysis of printed DNA microarray diagnostics is only possible if controlled and reliable spot uniformity (i.e., spot density, size, and shape repeatability) is achieved.

Currently, fluorescence imaging (scanner-based methods and microscopy) are the most commonly used techniques to analyze and quantify fluorescently labeled DNA patterns.⁵ Although fluorescence imaging involves routine instrumentation with well-developed techniques widely available, it also has several limitations. For example, fluorescence signal generation is very sensitive to variations in surface molecular environments and does not provide chemical or structural information at each stage of the patterning process. Variable fluorescent DNA labeling and differences in quantum yields with position, label type, and surface capture format all make accurate quantification difficult, and in general, chemical labeling of biological molecules with a fluorescent moiety can alter their natural activity, binding efficiency, and capture kinetics. Optical imaging methods such as surface plasmon microscopy (SPR)^{11–13} provide quantitative images of film thickness or molecular coverage but are generally insensitive to distinct chemical species present on the surface. Atomic force microscopy provides information about nanoscale topography and phase-segregated domains on a sample surface¹⁴ but provides little information on surface chemical composition.

X-ray photoelectron spectroscopy (XPS) and time-of-flight secondary ion mass spectrometry (TOF-SIMS) are two commonly used surface analysis techniques to characterize elements and molecules present in the top 2–10 nm of a surface,¹⁵ with detection limits as low as nanograms per square centimeter.¹⁶ XPS and TOF-SIMS each have their own strengths and weaknesses with respect to generating surface chemical state information at high spatial resolution, but used together they provide a powerful complementary set of techniques. The quantitative nature of XPS combined with its 2–10 nm sampling depth makes it an ideal technique for determining surface concentrations of biomolecules, including DNA.^{7,17–22} We have recently demonstrated that the XPS-determined phosphorus signal from the DNA backbone correlates well with ³²P-

radiolabeling¹⁹ and can be used to quantify both surface DNA probe and target concentrations.²³ Innovations in X-ray focusing and lens/analyzer technology now permit XPS imaging at spatial resolutions less than 10 μm .^{24–27} Although this spatial resolution remains orders of magnitude above that obtained with other microscopy techniques, XPS has significant advantages in quantifying sample surface composition. In contrast to imaging XPS, imaging TOF-SIMS is a more surface sensitive technique (1–2 nm sampling depth), providing significantly higher spatial resolution allowing more detailed analysis of compositional variability within a biomolecular pattern on solid substrates.^{28–30} Previous studies have shown that static TOF-SIMS, in combination with multivariate analysis statistical methods such as principal component analysis (PCA), can provide the distribution of chemical species across a patterned surface at sub-micrometer resolution.^{31,32}

In this study, complementary imaging XPS, imaging TOF-SIMS, and fluorescence imaging were compared, providing detailed characterization of chemical composition, spatial distribution, and hybridization efficiency of amine-terminated single-stranded DNA (ssDNA) probes bound to amine-reactive commercial microarray slides, immobilized in both macrospot and microarray formats. Fluorescence scanning shows intra- and interspot DNA density differences and heterogeneities. Combining imaging XPS and small spot analysis, we identified DNA microarray regions on the slide surface and quantified DNA elements within individual microarray spots. Imaging TOF-SIMS was used to provide unambiguous measurements of lateral DNA distribution within microspots. PCA was applied to TOF-SIMS imaging datasets demonstrating that combining these two techniques improves information yield not readily observable in the TOF-SIMS images alone, particularly in identifying species causing such common nonuniformities in DNA spots such as the “halo” or “donut” effects often observed in microarray fluorescence images.

Experimental Section

Materials. Ultrapure water (UPW) was used for all solution preparation and rinsing (ASTM type I water, 18.2 M Ω ·cm). High performance liquid chromatography (HPLC)-purified DNA oligomers (see Table 1) were purchased from TriLink Biotechnologies (San Diego, CA). All chemicals were used as received. Buffer salts, Tween20, sarcosine, sodium dodecyl sulfate (SDS), and ethanolamine were ACS grade or better and purchased from Sigma-Aldrich (St. Louis, MO). 1-(3-Dimethylaminopropyl)-3-ethylcarbodiimide (EDC) and *N*-hydroxysuccinimide (NHS) were purchased from Acros organics (98%+ purity; Morris Plains, NJ). Polymer-coated commercial amine-reactive, polyacrylamide-based microarray slides were purchased from GE Healthcare (CodeLink activated slides, Piscataway, NJ) and stored according to vendor recommendations until used. Figure S1 (Supporting

- (9) Peterson, A. W.; Heaton, R. J.; Georgiadis, R. M. *Nucleic Acids Res.* **2001**, *29*, 5163–5168.
- (10) Herne, T. M.; Tarlov, M. J. *J. Am. Chem. Soc.* **1997**, *119*, 8916–8920.
- (11) Piliarik, M.; Vaisocherova, H.; Homola, J. *Biosens. Bioelectron.* **2005**, *20*, 2104–2110.
- (12) Shumaker-Parry, J. S.; Aebersold, R.; Campbell, C. T. *Anal. Chem.* **2004**, *76*, 2071–2082.
- (13) Wolf, L. K.; Fullenkamp, D. E.; Georgiadis, R. M. *J. Am. Chem. Soc.* **2005**, *127*, 17453–17459.
- (14) Wadu-Mesthrige, K.; Xu, S.; Amro, N. A.; Liu, G. Y. *Langmuir* **1999**, *15*, 8580–8583.
- (15) Castner, D. G.; Ratner, B. D. *Surf. Sci.* **2002**, *500*, 28–60.
- (16) Wagner, M. S.; McArthur, S. L.; Shen, M. C.; Horbett, T. A.; Castner, D. G. *J. Biomater. Sci., Polym. Ed.* **2002**, *13*, 407–428.
- (17) Shen, G.; Anand, M. F. G.; Levicky, R. *Nucleic Acids Res.* **2004**, *32*, 5973–5980.
- (18) Lee, C. Y.; Canavan, H. E.; Gamble, L. J.; Castner, D. G. *Langmuir* **2005**, *21*, 5134–5141.
- (19) Lee, C.-Y.; Gong, P.; Harbers, G. M.; Grainger, D. W.; Castner, D. G.; Gamble, L. J. *Anal. Chem.* **2006**, *78*, 3316–3325.
- (20) Lee, C.-Y.; Gamble, L. J.; Grainger, D. W.; Castner, D. G. *Biointerphases* **2006**, *1*, 82–92.
- (21) May, C. J.; Canavan, H. E.; Castner, D. G. *Anal. Chem.* **2004**, *76*, 1114–1122.
- (22) Petrovykh, D. Y.; Kimura-Suda, H.; Whitman, L. J.; Tarlov, M. J. *J. Am. Chem. Soc.* **2003**, *125*, 5219–5226.

- (23) Gong, P.; Lee, C.-Y.; Gamble, L. J.; Castner, D. G.; Grainger, D. W. *Anal. Chem.* **2006**, *78*, 3326–3334.
- (24) Walton, J.; Fairley, N. *Surf. Interface Anal.* **2006**, *38*, 1230–1235.
- (25) Walton, J.; Fairley, N. *Surf. Interface Anal.* **2006**, *38*, 388–391.
- (26) Vohrer, U.; Blomfield, C.; Page, S.; Roberts, A. *Appl. Surf. Sci.* **2005**, *252*, 61–65.
- (27) Walton, J.; Fairley, N. *Surf. Interface Anal.* **2004**, *36*, 89–91.
- (28) Belu, A. M.; Yang, Z. P.; Aslami, R.; Chilkoti, A. *Anal. Chem.* **2001**, *73*, 143–150.
- (29) Yang, Z. P.; Belu, A. M.; Liebmann-Vinson, A.; Sugg, H.; Chilkoti, A. *Langmuir* **2000**, *16*, 7482–7492.
- (30) Belu, A. M.; Graham, D. J.; Castner, D. G. *Biomaterials* **2003**, *24*, 3635–3653.
- (31) Wagner, M. S.; Graham, D. J.; Castner, D. G. *Appl. Surf. Sci.* **2006**, *252*, 6575–6581.
- (32) Tyler, B. J. *Appl. Surf. Sci.* **2006**, *252*, 6875–6882.

Table 1. Oligonucleotide Sequences and Terminal Modifications

DNA	identifier	5'-modification	sequence	3'-modification
complementary probe ^{a,b}	oligo1-NH ₂		CTGAACGGTAGCATCTTGAC	-C ₆ -NH ₂
complementary probe ^{a,b}	Cy3-oligo1-NH ₂	Cy3-C ₆ -	CTGAACGGTAGCATCTTGAC	-C ₆ -NH ₂
noncomplementary probe ^a	oligo3-NH ₂		GTCAAGATGCTACCGTTCAG	-C ₆ -NH ₂
target ^{a,b}	oligo2		GTCAAGATGCTACCGTTCAG	
target ^{a,b}	Cy5-oligo2	Cy5-C ₆ -	GTCAAGATGCTACCGTTCAG	
brominated target ^{a,b,c}	Br-oligo2		GTCAAGATGCTACCGTTCAG	

^a Used in microarray printing. ^b Used in hand printing of macrospots. ^c The first 10 nucleotides at the 5' end were brominated.

Information) shows chemical structures for the various additives used in the DNA printing and hybridization.

Macrospot DNA Probe Immobilization. DNA oligonucleotides containing a 3'-terminal hexylamine group (see Table 1) were spotted onto activated CodeLink microarray slides. Briefly, slides were removed from vendor packaging and directly activated using standard carbodiimide chemistry with EDC/NHS according to a previously published protocol³³ to ensure maximal and reliable amine reactivity. Slides were then spotted with DNA solutions using a pipet (hand-spotting; 10 μ L/spot) yielding defined macrospotted DNA areas of approximately 5 mm in diameter.⁷ DNA solutions (Cy3-oligo1-NH₂:oligo1-NH₂, 1:99) were spotted at 0, 1, 10, 20, and 40 μ M in print buffer (150 mM sodium phosphate, pH 8.5 containing 0.001% Tween20 and 0.001% sarcosine). To minimize variations due to spot location, each DNA concentration was spotted in triplicate randomly across the slide. Hand-spotted samples were incubated overnight (> 13 h) at 75% relative humidity, permitting drying to yield DNA film spots with immobilized density similar to microarray preparations.⁷

Microarray Printing. Oligonucleotides containing a 3'-terminal hexylamine group (Table 1) were printed onto activated³³ CodeLink microarray slides using a noncontact Piezarray printer (Perkin-Elmer equipped with standard Perkin-Elmer piezarray pins and driven by Piezarray Microarray Printing System Version 1.1 software). Complementary (Cy3-oligo1-NH₂:oligo1-NH₂, 1:99) and noncomplementary (oligo3-NH₂) DNA probe solutions were deposited from print buffer volumes of $\sim 333 \pm 33$ pL (10% deviation) in replicates of 10 in alternating rows (layout of the printed microarray regions can be found in Figure S2, Supporting Information). Four different probe concentrations (0, 10, 20, and 40 μ M) were used for microarray printing, with each array representing a single printed probe concentration. Duplicate arrays were printed on separate slides to allow comparison between probe-only and hybridized arrays (4 arrays/slide). Humidity during printing was approximately 60%. Under these print conditions, spots dry immediately to produce dried spot diameters of approximately 150 microns. Printed slides were incubated overnight (>13 h) at room temperature under 75% relative humidity.

Postprint Treatment and Hybridization with Target DNA. After printing and incubation, slides were treated according to the manufacturer's recommendations. Slides were rinsed briefly with print buffer followed by UPW and then immersed in blocking solution (50 mM ethanolamine in 0.1 M Tris, pH 9.0) at 50 °C for 30 min to consume residual amine-reactive groups. Following blocking, slides were rinsed 3 times with UPW and then washed with 4X saline sodium citrate (SSC) containing 0.1% SDS at 50 °C for 30 min (1X SSC: 15 mM sodium citrate and 150 mM NaCl). After washing, slides were rinsed 3 times with UPW and finally blown dry with nitrogen. Target hybridization was accomplished using either Lifterslips (Erie Scientific no. 22x50I-2-4711) or Coverwell perfusion chambers (Grace Bio-Labs no. PC4L-A-1.0) for macrospot and microarray samples, respectively. Briefly, 1 μ M target DNA solution (1:99 Cy5-Oligo2:Br-Oligo2 or 1:99 Cy5-Oligo2:Oligo2) prepared in hybridization buffer (4X SSC/0.01% SDS) was applied to the appropriate hybridization chamber for 4 h at room temperature and at 100% relative humidity. Following hybridization, slides were rinsed once with hybridization buffer, twice with 2X SSC/

Table 2. Compiled XPS Compositional Data for Noncontact Printed Microarrays and Hand-Spotted DNA Macrospots on CodeLink Slides

sample	atomic % (SD)							
	P 2p	N 1s	Si 2p	O 1s	C 1s	Na 1s	Ca 2p	Cl 2p
fresh, unmodified slide	0.0 (0.0)	8.8 (0.1)	7.5 (0.3)	28.7 (0.3)	53.3 (0.5)	1.1 (0.1)	0.5 (0.0)	0.0 (0.0)
Microarray DNA								
printing buffer + blocking	0.0 (0.0)	7.6 (0.5)	8.8 (0.5)	30.5 (1.5)	50.6 (1.4)	1.1 (0.3)	0.6 (0.2)	0.0 (0.0)
probe (40 μ M) + blocking	1.3 (0.2)	11.8 (1.1)	5.4 (0.4)	25.7 (0.8)	52.7 (1.0)	3.1 (0.7)	0.0 (0.0)	0.0 (0.0)
probe (40 μ M) + blocking + target (1 μ M)	2.2 (0.1)	13.1 (0.9)	3.3 (0.4)	23.0 (1.7)	52.8 (2.5)	5.6 (0.6)	0.0 (0.0)	0.0 (0.0)
Macrospot DNA								
printing buffer + blocking	0.0 (0.0)	7.8 (0.9)	8.3 (0.5)	30.0 (0.7)	52.9 (1.3)	0.5 (0.2)	0.5 (0.1)	0.0 (0.0)
probe (40 μ M) + blocking	0.5 (0.1)	10.5 (0.8)	6.3 (0.5)	27.2 (0.6)	54.0 (0.6)	1.0 (0.4)	0.5 (0.1)	0.0 (0.0)
probe (40 μ M) + blocking + target (1 μ M)	1.0 (0.1)	10.7 (0.6)	5.3 (0.7)	26.8 (1.2)	51.8 (1.6)	3.1 (0.3)	0.3 (0.2)	1.1 (0.2)

0.1% SDS (5 min each), once with 0.2X SSC (1 min), once with 4 °C 0.1X SSC, and finally dried with nitrogen. All probe-only control spots were exposed to identical hybridization buffer and subsequent rinse steps. For macrospot probe samples, the final rinse was UPW.

Fluorescence Imaging of Macrospot and Microarray Surfaces. Modified slides were scanned using a ScanArray Express Microarray Imager (Perkin-Elmer, Fremont, CA) with scanning resolutions of 10 μ m for microarray samples and 50 μ m for macrospot samples. Slides were scanned using two channels, 543 and 633 nm, for Cy3- and Cy5-labeled samples, respectively.⁷ Laser power was set to 90% for all scans. For microarray samples, PMT sensitivity was set to 75% and 50% for probe and target measurements, respectively. For macrospot samples, PMT sensitivity was set to 62% and 50% for probe and target measurements, respectively. High-resolution fluorescent images were acquired using an inverted Nikon TE2000U microscope equipped with a Sutter Lambda LS xenon source, a Prior scientific XYZ-stage, Chroma excitation/emission filters, and a Photometrics scientific CCD camera (Coolsnap-ES) controlled by Metamorph software (v.6.2r6, Molecular Devices, Downingtown, PA). Microarray spots were analyzed using the ScanArray software as previously described.⁷ Macrospot samples were analyzed using ImageQuant software (Amersham Biosciences, v. 5.1) using grayscale image analysis. The use of separate software for analysis of the macrospots was necessary due to the inability of the ScanArray software to handle millimeter-size spots.

XPS Analysis of DNA Macrospot and Microarray Surfaces. All XPS measurements were performed on a Kratos Axis Ultra DLD X-ray photoelectron spectrometer employing a hemispherical analyzer for spectroscopy and a spherical mirror analyzer for imaging.²⁴ Spectra and images were acquired with a monochromated Al K α X-ray source and a 0° takeoff angle (TOA) in the "hybrid" mode. The TOA is defined as the angle between the sample surface normal and the axis of the

(33) Gong, P.; Grainger, D. W. *Surf. Sci.* **2004**, *570*, 67–77.

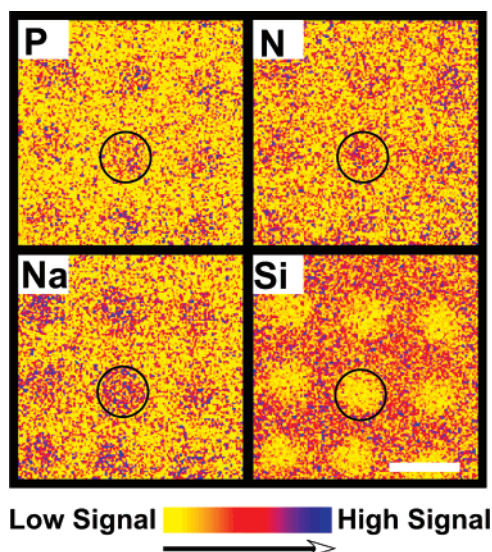


Figure 1. XPS elemental images ($800\ \mu\text{m} \times 800\ \mu\text{m}$) of aminated DNA probes printed onto CodeLink microarray slides at $40\ \mu\text{M}$ DNA concentration. While phosphorus is unique to DNA, silicon is unique to the substrate. In combination, these elemental images enable unambiguous identification of the spatial distribution of DNA for XPS region of interest (ROI) compositional analyses of the printed DNA microarray spots. The scale bar represents $200\ \mu\text{m}$.

XPS analyzer lens. A low-energy electron flood gun was used to minimize surface charging.

XPS data for macrospot DNA samples were collected using an analysis area of $700\ \mu\text{m} \times 300\ \mu\text{m}$. For each sample, an initial compositional survey scan was acquired, followed by a detailed P2p scan using a pass energy of 80 eV. High-resolution C1s spectra were also acquired for the fresh, unmodified CodeLink slides using a pass energy of 20 eV and were charge-referenced to the C1s hydrocarbon peak set to 285.0 eV. Values reported for the composition of fresh CodeLink slides, and the DNA macrosamples were averages of values determined from three spots on two CodeLink microarray slides.

DNA spots on each microarray sample were located by taking initial XPS images of the relevant species (P2p, N1s, O1s, C1s, and Si2p). Images were acquired at $400 \times 400\ \mu\text{m}$ and $800 \times 800\ \mu\text{m}$ fields of views at a pass energy of 80 eV. Background region images were taken at a binding energy 15 eV below each relevant peak. Background corrected images were obtained by subtraction of the background region image from the image at the peak of interest.²⁶ Compositional analysis of individual microarray DNA spots was performed by collecting small-area region of interest (ROI) scans ($50\ \mu\text{m} \times 50\ \mu\text{m}$) from the center of individual microarray spots. ROI spectra were acquired from a $400\ \mu\text{m}$ field of view using an aperture size of $55\ \mu\text{m}$. An initial compositional survey scan was acquired at the specified location, followed by detailed (P2p) scans using a pass energy of 160 eV. Four to six DNA spots from each 10×10 array were analyzed. Reported compositional data were averages of values determined from replicate spots. Data analysis was performed with Vision Processing data reduction software (Kratos Analytical Ltd.) and CasaXPS (Casa Software Ltd.).

TOF-SIMS Analysis of DNA Microarray Surfaces. TOF-SIMS data were acquired on an ION-TOF IV instrument (ION-TOF GmbH, Münster, Germany, University of Oregon) using a Bi^+ primary ion source. Positive and negative ion images and spectra were acquired with a pulsed 25 keV, 1.3 pA primary ion beam in high current bunched mode from $200\ \mu\text{m} \times 200\ \mu\text{m}$ areas on sample surfaces. All images obtained contained 128×128 pixels. These analysis conditions resulted in a spatial resolution of approximately $2\ \mu\text{m}$. Data were collected using an ion dose below the static SIMS limit of 1×10^{12} ions/cm². A low-energy electron beam was used for charge compensation on the DNA

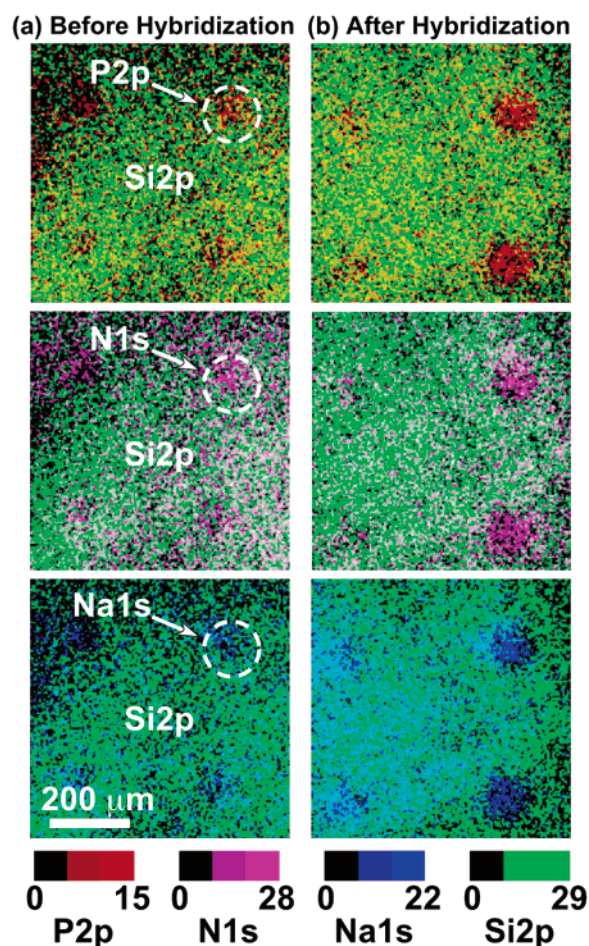


Figure 2. XPS overlay of phosphorus (P2p), nitrogen (N1s), sodium (Na1s) with the substrate silicon (Si2p) signal intensity images ($800 \times 800\ \mu\text{m}$) from printed DNA probes on CodeLink microarray slides (a) before and (b) after target hybridization. Consistent with target capture signal, the XPS P2p, N1s, and Na1s signal intensities from the hybridized regions are significantly higher than those from the unhybridized regions.

samples. The mass resolutions ($m/\Delta m$) for the negative spectra were typically between 6000 and 7500 for the (m/z) 25 peaks in the negative spectra. Positive spectra were not used due to high sodium ion intensity from buffer salt–DNA ion exchange; this is a problem resulting from the inability to perform a final water rinse to remove counterions and trapped Na within the CodeLink matrix without also disrupting the hybridization. Principal component analysis (PCA) was performed on TOF-SIMS data as described previously^{31,34} using a series of scripts written by NESAC/BIO for MATLAB (MathWorks, Inc., Natick, MA) (see Supporting Information for a detailed description of PCA).

Results and Discussion

XPS Analysis of Surface-Immobilized and Hybridized DNA on Commercial Microarraying Substrates: Microarray vs Macrospot Format. Surface compositions of noncontact printed microarray spots ($100\text{--}150\ \mu\text{m}$ diameter) and hand-printed macrosamples ($\sim 5\ \text{mm}$ diameter) were analyzed by XPS for direct comparison of DNA probe immobilization and hybridization efficiencies on CodeLink slides. The slide polymer chemistry has been reported elsewhere^{7,8} and verified here by XPS to be consistent with polyacrylamide containing activated ester groups as attachment sites for aminated DNA probes. XPS

(34) Wickes, B. T.; Kim, Y.; Castner, D. G. *Surf. Interface Anal.* **2003**, *35*, 640–648.

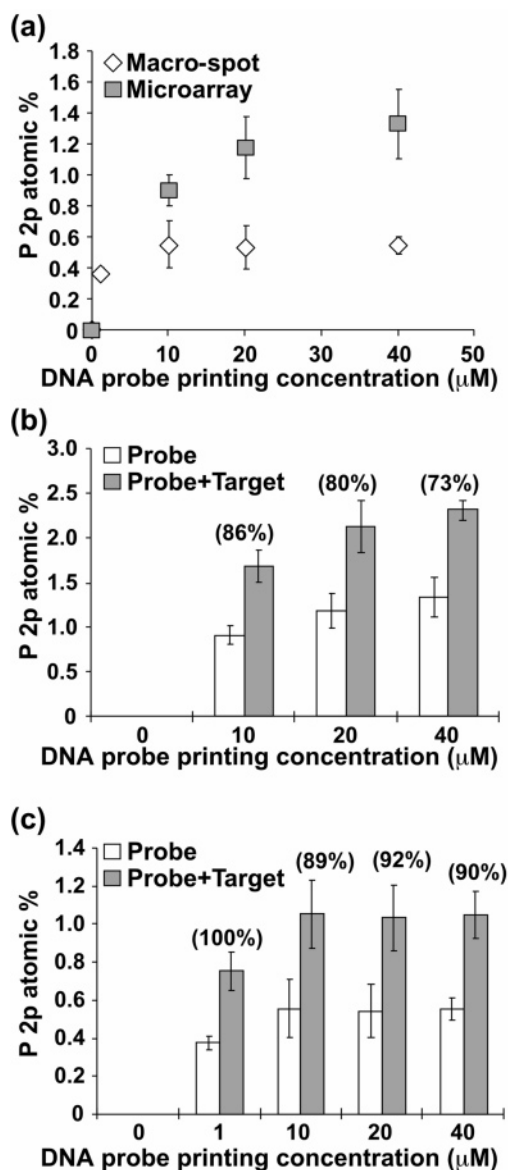


Figure 3. Relative amounts of DNA probe immobilized onto CodeLink slides are compared in microarray and macrospot formats (a). Amounts of DNA on CodeLink surfaces are proportional to P2p atomic percent (atom %).⁷ Hand-spotted macrospot printing concentrations are 1, 10, 20, and 40 μM (150 mM sodium phosphate, pH 8.5). Microarrays were printed at three DNA probe concentrations (10, 20, and 40 μM) under the same printing conditions as those for the macrospot DNA. Target hybridization efficiencies for the microarray (b) and macrospots (c) shown in parentheses above each concentration were derived as a percentage of probe molecules hybridized $[\frac{((\text{P}2\text{p atom \% of hybridized spot}/\text{P}2\text{p atom \% of probe spot}) - 1) \times 100\%]}{((\text{P}2\text{p atom \% of hybridized spot}/\text{P}2\text{p atom \% of probe spot}) - 1) \times 100\%}]$. The P2p atomic % shown in this figure and used for hybridization efficiency calculations have been renormalized excluding the Na signal since rinsing in pure water to remove salts could not be done on the hybridized samples. Hybridization efficiency slightly above 100% was rounded to 100%.

compositional data of the fresh, as received, microarray slides indicate the presence of silicon, carbon, nitrogen, oxygen, and trace ions (calcium and sodium) throughout the substrate surface (Table 2). The XPS C1s high-resolution spectrum of the unmodified microarray slide shows 70% C–C and C–H at 285 eV, 8% C–O and C–N at 286 eV, and 22% N–C=O at 288 eV, similar to those published previously for Codelink slides⁷ and pure polyacrylamide³⁵ but deviating slightly due to the

(35) Garg, D. H.; Lenk, W.; Berwald, S.; Lunkwitz, K.; Simon, F.; Eichhorn, K. *J. Appl. Polym. Sci.* **1996**, *60*, 2087–2104.

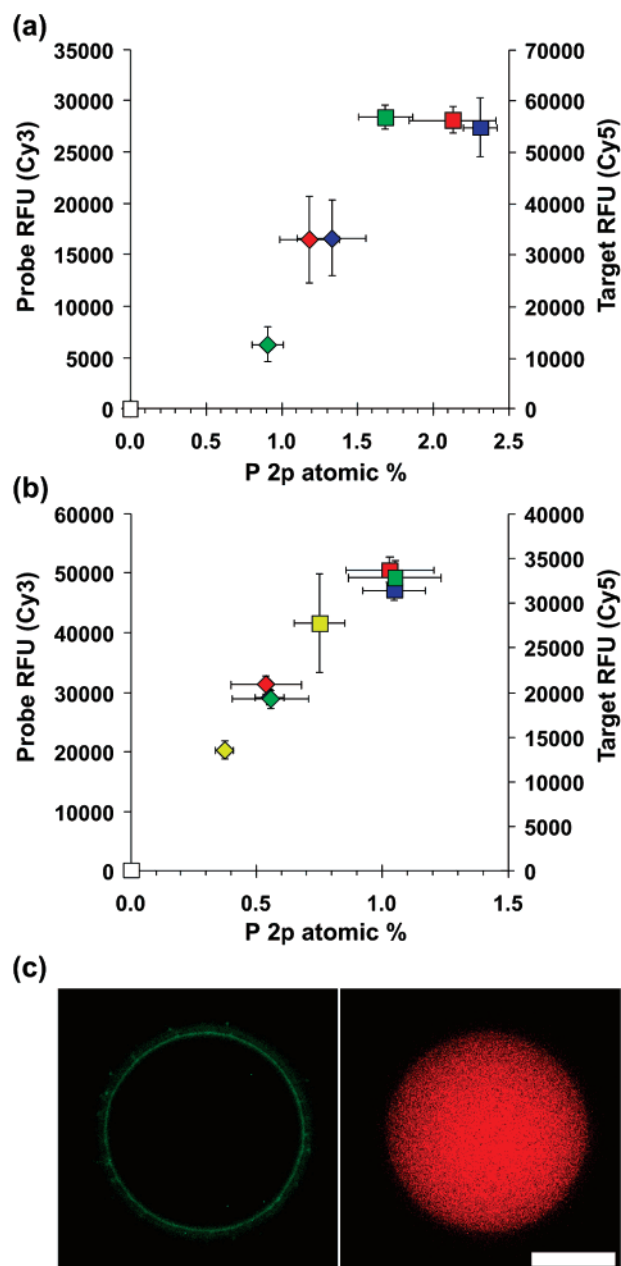


Figure 4. Correlation between P 2p atomic % from XPS and relative fluorescence units (RFU) data collected from microarray printed (a) and hand-spotted (b) samples. (c) Fluorescent image of printed probe (left) and hybridized target (right) collected using a fluorescent microscope showing a “halo effect”; scale bar represents 50 μm . For this analysis, all samples were incubated at 75% humidity overnight to facilitate probe covalent attachment. Symbol key: diamonds, probe; squares, target. Probe concentration key: white, 0 μM ; yellow, 1 μM ; green, 10 μM ; red, 20 μM ; blue, 40 μM .

detection of the underlying glass substrate signal (for more details see Figure S3, Supporting Information).

XPS imaging combined with small-spot ROI analysis was used to provide quantitative surface composition for the microarrays immobilized with 0, 10, 20, and 40 μM DNA probe concentrations and then hybridized with 1 μM DNA target. Importantly, the 0 μM (blank) concentration represents experimental controls of buffer-printed microarray slides exposed to identical incubation, post-immobilization wash, and hybridization steps as the DNA-modified samples, but in the absence of DNA probes. Figure 1 presents, to our knowledge, the first

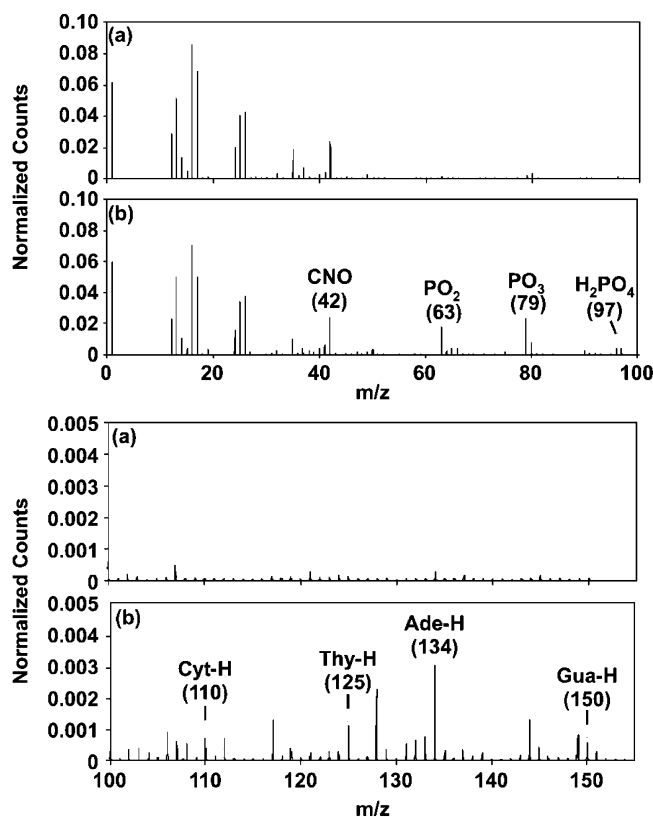


Figure 5. Negative ion TOF-SIMS ROI spectra from the (a) substrate and (b) DNA regions of the microarray surface. The DNA region shows characteristic nucleic acid peaks at m/z 42 (CNO⁻), 63 (PO₂⁻), 79 (PO₃⁻), 97 (H₂PO₄⁻), 110 (C₄H₄N₃O⁻, Cyt-H), 125 (C₅H₅N₂O₂⁻, Thy-H), 134 (C₅H₄N₅⁻, Ade-H), and 150 (C₅H₄N₅O⁻, Gua-H) that were absent or present at much lower intensities in the background substrate region.

reported XPS elemental images (P, N, Na, and Si) from individual spots in DNA microarrays (O and C images not shown). Background corrected P2p images (Figure 1) show higher signal intensity in the areas occupied by immobilized DNA microspots. Although N, Na, and Si are present throughout the substrate surface, higher N1s and Na1s and lower Si2p signal intensities were also observed in the areas covered by the DNA microspots. Higher N and Na signal intensities correlate with nitrogen-containing DNA bases and sodium counterions associated with the DNA polyphosphate backbone. DNA coverage in printed regions attenuates absolute signal intensity (i.e., Si) from the underlying glass substrate. In addition, XPS imaging provides the capability to distinguish between hybridized and unhybridized microspots on a commercial microarray slide without use of radioactive or fluorescent labels. Figure 2 shows XPS overlay images displaying P, N, Na, and Si signal intensities from a hybridized (Figure 2a) and an unhybridized (Figure 2b) microarray slide. Prior to exposing the microarray slide to complementary target capture, similar XPS P2p, N1s, and Na1s signal intensities were detected from all microspots containing complementary or noncomplementary probe sequences. After target hybridization, microspots containing complementary probe sequences exhibited higher XPS P2p, N1s, and Na1s signal intensities compared to those containing noncomplementary probe sequences, as expected.

To further determine target hybridization efficiencies for microarrays printed at various printed probe concentrations (e.g.,

10, 20 and 40 μ M), small area ROI analyses were performed on microspots to obtain quantitative individual spot DNA elemental compositions both before and after hybridization. Consistent with XPS elemental images (e.g., Figure 2), regions with hybridized DNA targets show higher percentages of phosphorus (2.2 atomic percent or atom %), nitrogen (13.1 atom %), and sodium (5.6 atom %) and lower substrate oxygen (23.0 atom %) and silicon (3.3 atom %) signals compared to that obtained for unhybridized noncomplementary probe spots (P = 1.3, N = 11.8, Na = 3.1, O = 25.7 and Si = 5.4 atom %, Table 2). Since substantial amounts of nitrogen (~8 atom %) are present in the unprinted CodeLink polymer layer,⁷ DNA phosphorus is the only unique characteristic element useful to quantify relative amounts of surface-immobilized and hybridized DNA oligomers from the various probe printing concentrations. DNA surface coverage is proportional to phosphorus atomic concentration and has been previously reported as a quantification method for immobilized DNA on gold^{22,23} as well as on polymer-modified silicon substrates.^{7,17} Figure 3a and b show relative amounts of surface-immobilized probe and hybridized DNA obtained for each probe printing concentration from small area XPS analysis. As seen in Figure 3a, P2p atom % from the DNA microspots increases with increasing spotting probe solution concentration and did not saturate for the concentration range investigated. Target hybridization efficiencies shown in parentheses above each concentration in Figure 3b were derived from the P2p signal as a percentage of probe molecules hybridized [$((P2p \text{ atom \% of hybridized spot}/P2p \text{ atom \% of probe spot}) - 1) \times 100\%$]. A hybridization efficiency of 86% was obtained for microspots printed at the lowest probe concentration of 10 μ M. At higher probe printing concentrations (20 and 40 μ M), slightly lower hybridization efficiencies (80% and 73%) were obtained. The reduction of hybridization efficiency at higher probe coverage has been reported previously,^{7,9,23} explained by steric and electrostatic crowding effects in closely packed DNA probes that hinder DNA target duplex formation on the surface.³⁶

One key difference between robotic microarray spotting and bulk media surface immobilization (i.e., large area hand-spotting or solution-phase capture) is the effect of probe spot drying. Microarray printing delivers nanoliter drops of DNA solution to the assay surface that evaporate within seconds, minimizing opportunities for equilibrium DNA covalent reactions with the surface and yielding a dried DNA aggregated film. This rapid evaporative process therefore produces substantially different DNA immobilization states in spots compared to slow-drying or nondrying bulk media reactions.⁷

To compare immobilized probe and hybridized target densities obtained from these two different printing methods, DNA probes were hand-printed in macrospot formats (~5 mm diameter) using the same printing conditions as those for the microarrays and analyzed by XPS. XPS compositional data for the macrospots are summarized in Table 2 and Figure 3a and c. Reduced DNA (P and N) and increased substrate (Si and O) signals were detected from macrospots versus microarrays for the same probe printing concentrations (Table 2). Figure 3a shows that lower percentages of phosphorus, indicative of DNA surface density, were observed for macrospots over the entire probe

(36) Heaton, R. J.; Peterson, A. W.; Georgiadis, R. M. *Proc. Natl. Acad. Sci. U.S.A.* **2001**, *98*, 3701–3704.

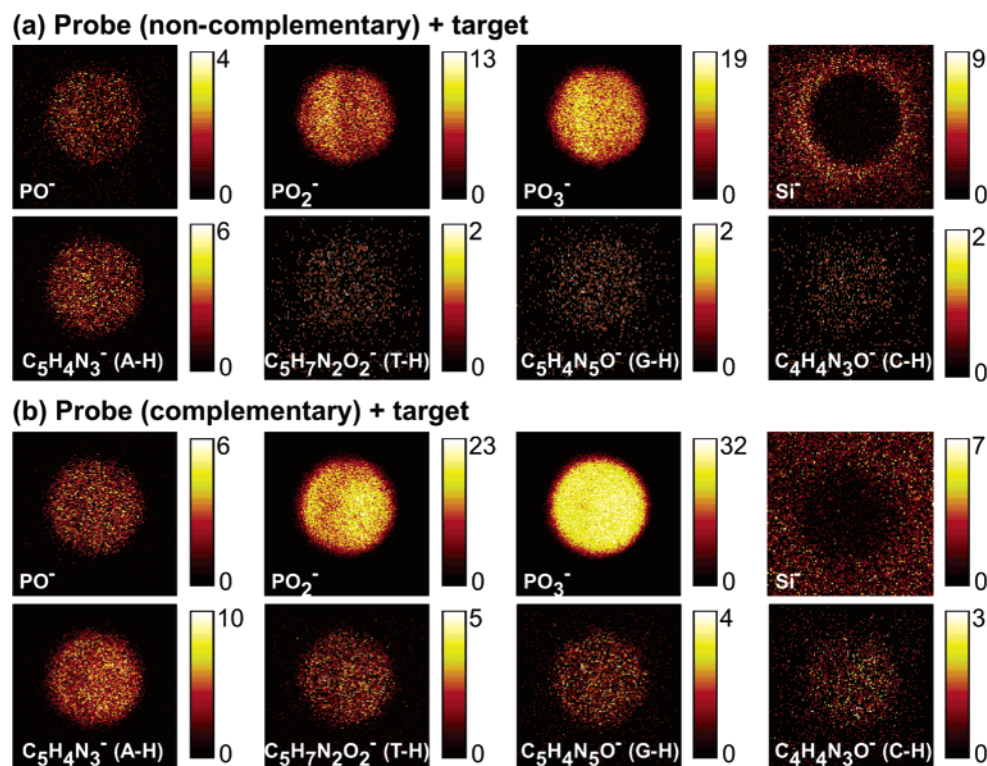


Figure 6. Representative negative ion TOF-SIMS images showing the distribution of DNA and substrate fragments within a single (a) unhybridized and (b) hybridized microarray spot. The DNA fragments are localized to the noncontact printed regions but distributed inhomogeneously within the microspot. The Si image from the unhybridized probe spot (a) showed a “halo” feature around the spot. Brighter pixel intensity corresponds to higher DNA or substrate signals (counts per pixel). Images are $200\ \mu\text{m} \times 200\ \mu\text{m}$.

printing concentration range ($0\text{--}40\ \mu\text{M}$). Amounts of immobilized probe in macrosites saturate at $10\ \mu\text{M}$ probe solution concentration. Observed differences in amounts of immobilized DNA between macro- and microspot formats can be explained by different spot drying rates.⁷ Rapid evaporation during microarray printing significantly increases ionic strength of the spotting buffer as well as DNA concentration, promoting higher DNA probe surface immobilization density.⁷ Target hybridization increases the percentage of phosphorus and nitrogen on macrosites while decreasing the oxygen and silicon substrate signals, as observed with DNA microarrays (Table 2). Lower probe density on the macrosites reduces steric and electrostatic problems on the surface, yielding higher hybridization efficiencies (Figure 3c). A hybridization efficiency of 100% was obtained on the lowest probe concentration regions (DNA spotting concentration of $1\ \mu\text{M}$). At the higher probe spotting concentrations ($10\text{--}40\ \mu\text{M}$), a small reduction in target hybridization efficiency ($\sim 90\%$) is again observed.

Fluorescence Analysis of Surface-Immobilized and Hybridized DNA. Printed slides were compared using a fluorescence scanner to provide complementary, more conventional information regarding relative density and homogeneity of probes and targets in microarray and macrosites. Figure 4a and b show correlations between the relative fluorescence signal (Cy3 probe and Cy5 target) and XPS P2p atom % (shown in Figure 3) for microarray and macrosite samples. Data show reasonable correlations between RFUs and P2p atom %, both representative of immobilized or hybridized oligo densities. Under current experimental conditions (e.g., standard 75% humidity), large variations in fluorescence intensity in the 20--

$40\ \mu\text{M}$ range (hand-spotted) and $10\text{--}40\ \mu\text{M}$ range (printed array) were absent due to spot solution evaporation as discussed above. At $1\ \mu\text{M}$ coupling concentration (hand-spotting, Figure 4b) macrosite RFUs were different compared to those for higher coupling concentrations. Although XPS results for hand-spotted macrosite data agree well with fluorescence measurements, XPS proved to be more sensitive to variations in probe density for microspots compared to fluorescence measurements. Additionally, fluorescence measurements provide relative, qualitative assessment of hybridization efficiencies, while XPS provides quantitative % efficiencies. Hand-spotted samples incubated overnight at 100% humidity to better duplicate bulk immobilizations where evaporation effects are absent produced a much greater dependence of resulting RFU on coupling concentration as previously shown⁷ (data not shown). This is likely due to a combination of bulk phase aqueous hydrolysis and neutralization of surface reactive ester groups and diffusion-limiting DNA-surface coupling reactions.^{7,33}

Unlike XPS, fluorescence measurements can provide high-resolution area information about the homogeneity of array spots as seen in Figure 4c. The halo effect shown in Figure 4c is much more prevalent when using higher resolution fluorescence microscopy compared with standard fluorescent scanning or imaging XPS. XPS is able to detect and quantify total probe surface presence but is unable to resolve the 1% Cy3-labeled probe doped into the probe print solution. High-resolution fluorescence images show that this 1% Cy3-labeled probe has segregated to the spot periphery producing the observed fluorescent halo effect. However, from the uniform target hybridization fluorescent image, it is clear that although the 1% labeled probe resides at the periphery, the printed spot has active,

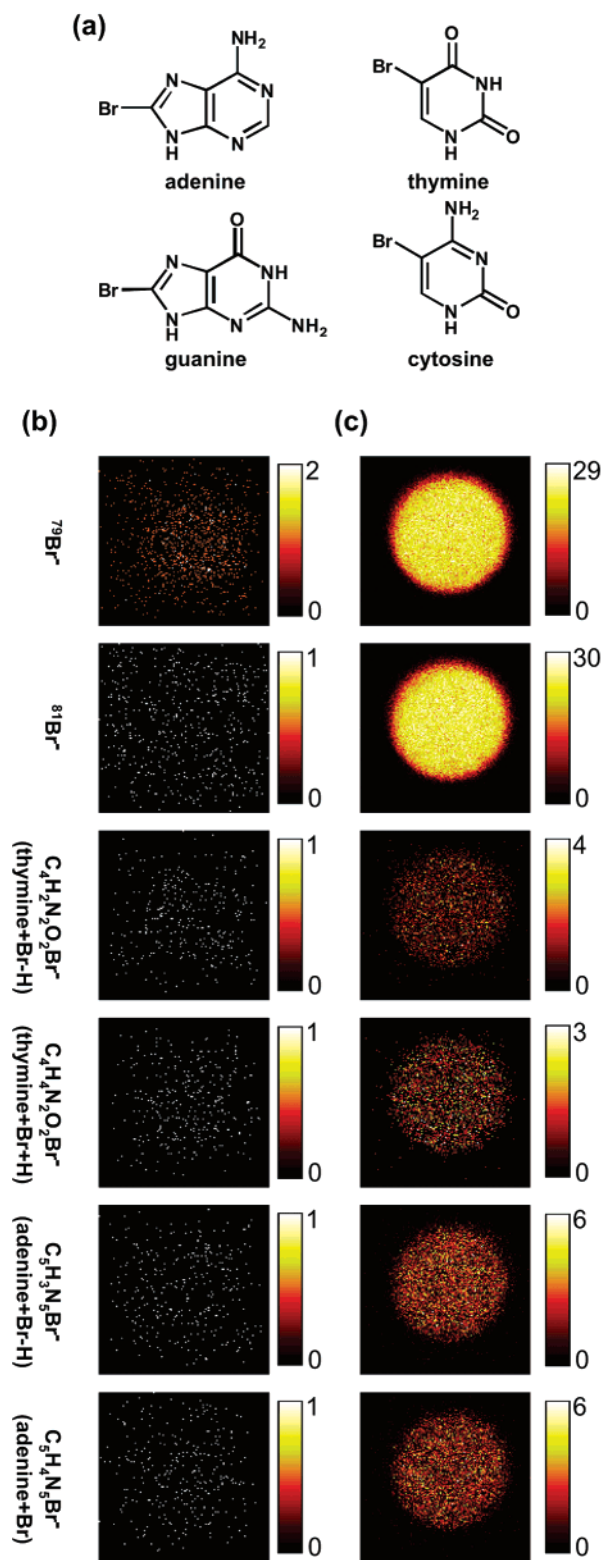


Figure 7. (a) Bromine modification of DNA target (50% brominated DNA bases comprise the DNA target sequence). Representative negative ion TOF-SIMS images showing no Br fragments detected from the noncomplementary (unhybridized) microspots (b). Microarrays exposed to Br-modified DNA targets produce strong Br signals for complementary (hybridized) microspots after target hybridization (c). Brighter pixel intensity corresponds to higher DNA or substrate signals (counts per pixel). Images are $200\ \mu\text{m} \times 200\ \mu\text{m}$.

unlabeled probe immobilized throughout its area. At this time we do not have a satisfactory explanation for the observed effect.

However, we will show in a related study that the amount of Cy3-labeled probe doped into the probe print solution (0 to 100%) dramatically affects spot homogeneity as examined using fluorescence microscopy. Given these results, the practice of doping a fluorescent probe into unlabeled probe at low concentrations to reduce the amount of the more expensive fluorescently labeled oligo may produce unrepresentative images of arrays when scanned, thus making interpretation difficult. Observation of halo or donut features in many printed microarrays^{8,33} has confounded microarray fluorescence analysis and data interpretation.^{37,38} Reasons for these defective printed features are not elucidated. Therefore, to determine if the observed fluorescence halo was correlated to specific molecules in the print solution, imaging TOF-SIMS was utilized to examine individual microspots.

TOF-SIMS Analysis of Microarray Spot Uniformity. TOF-SIMS was used to characterize the distribution of DNA molecules within individual DNA microspots via detection of the characteristic DNA ion fragments (i.e., DNA bases and phosphate backbone).^{18,21,39,40} Negative ion TOF-SIMS ROI spectra from the substrate and from DNA microspotted regions are shown in Figure 5a and b. The negative ion spectra from the DNA region (Figure 5b) show DNA phosphate fragments (PO^- , PO_2^- , PO_3^- , and H_2PO_4^-) at m/z 47, 63, 79, and 97, respectively.^{18,21,39,40} DNA bases, including adenine (Ade-H, m/z = 134), thymine (Thy-H, m/z = 125), guanine (Gua-H, m/z = 150), and cytosine (Cyt-H, m/z = 110), were also detected by TOF-SIMS in negative ion mode.^{18,21} The absence of these peaks in the negative spectra from the unspotted substrate region (Figure 5a) confirms their origin from surface-immobilized DNA molecules. Individual negative ion TOF-SIMS images from selected masses reveal the distribution of printed DNA within an unhybridized microspot containing noncomplementary DNA probes (Figure 6a) and a hybridized microspot containing complementary probes (Figure 6b) from the microarray region printed with $40\ \mu\text{M}$ DNA solution. The detectable spot diameter from the TOF-SIMS PO_x^- images was approximately $150\ \mu\text{m}$, comparable to that observed using fluorescence microscopy after printing (Figure 4c). These TOF-SIMS images, acquired at a spatial resolution of approximately $2\ \mu\text{m}$, indicate that printed DNA molecules are distributed nonuniformly within individual microarray spots upon drying. In addition, TOF-SIMS Si images of the unhybridized microspots reveal “halo” features around the probe spot consistent with those seen in fluorescent images (Figure 4c). (PCA analysis of these “halos” is presented later in this paper.) Also consistent with XPS data, images for characteristic DNA fragments (m/z 47, 63, 79, 97, 110, 125, 134, and 150) show higher signal intensities for the hybridized DNA microspot (Figure 6b).

TOF-SIMS was also used to identify DNA hybridization signal by hybridizing a complementary target sequence having 50% of the DNA bases each modified with one Br atom (Table 1 and Figure 7a). Printed probe microarrays exposed to Br-modified DNA complementary targets produced strong Br

(37) Li, Q. H.; Fraley, C.; Bumgarner, R. E.; Yeung, K. Y.; Raftery, A. E. *Bioinformatics* **2005**, *21*, 2875–2882.

(38) Tran, P. H.; Peiffer, D. A.; Shin, Y.; Meek, L. M.; Brody, J. P.; Cho, K. W. *Nucleic Acids Res.* **2002**, *30*.

(39) Hellweg, S.; Jacob, A.; Hoheisel, J. D.; Grehl, T.; Arlinghaus, H. F. *Appl. Surf. Sci.* **2006**, *252*, 6742–6745.

(40) Hashimoto, H.; Nakamura, K.; Takase, H.; Okamoto, T.; Yamamoto, N. *Appl. Surf. Sci.* **2004**, *231–2*, 385–391.

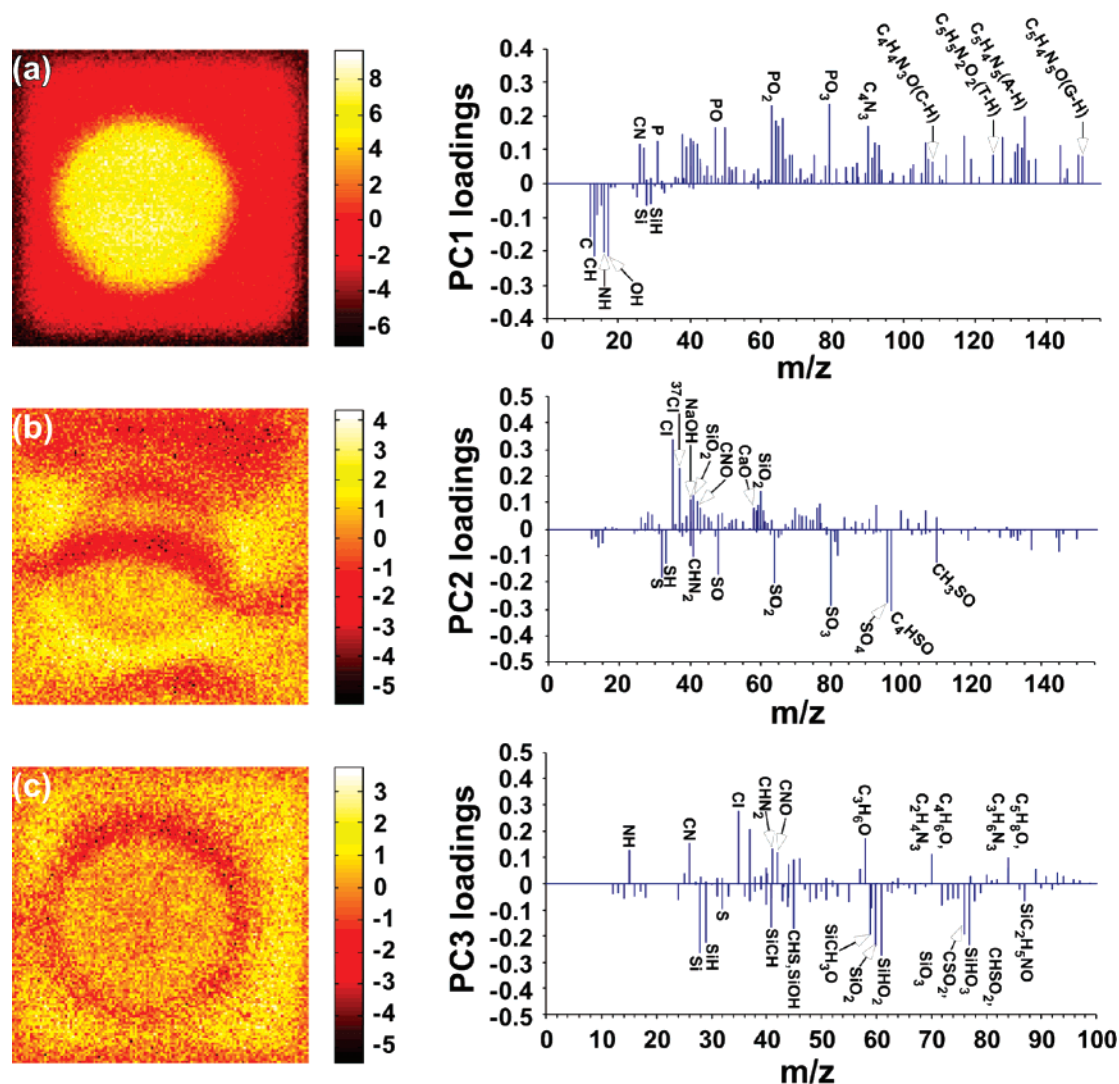


Figure 8. Image scores and loadings for PC 1 (a), PC 2 (b), and PC 3 (c) for an unhybridized microspot (negative ion images). PC 3 loadings (c) from the negative TOF-SIMS image data matrix indicate that the “halo” feature detected in spots by TOF-SIMS imaging is characterized by Si-containing fragments from the polymer-coated glass substrate. Images are $200\ \mu\text{m} \times 200\ \mu\text{m}$.

signals from hybridized probe spots (Figure 7b and c) compared to noncomplementary Br-containing targets (controls). TOF-SIMS’ intrinsic high sensitivity in detecting brominated species, as well as the ability to acquire images with submicron spatial resolution, opens the possibility to exploit this analytical method to determine hybridization uniformity across single microarray spots.

In addition to the DNA molecular fragments identified above, the energetic SIMS process yields hundreds of peaks in the 0–200 m/z range, making the interpretation of TOF-SIMS data difficult. To simplify data interpretation and identify image features related to other chemical species (e.g., salt ions, detergent molecules, polymer layer, etc.; for more details see Figure S1, Supporting Information), a multivariate analysis technique, PCA, was used for more detailed analyses of the TOF-SIMS images as described in the Supporting Information section.^{31,34} PCA was performed on the TOF-SIMS negative ion image of the unhybridized DNA microspot shown in Figure 6a to gain a better understanding of the chemical species related to the halo feature. The first three image scores and loadings from PCA are shown in Figure 8a, b, and c. Principal component 1 (PC 1, Figure 8a) clearly distinguishes the image features that

correspond to the DNA microspot (bright regions) and the substrate (dark regions). From the PC 1 loadings plot (Figure 8a) we confirmed that most major peaks with positive PC 1 loadings are associated with the microspot region in the TOF-SIMS images and are phosphate- and nitrogen-containing DNA fragments, while most major peaks with negative PC 1 loadings are hydrocarbon fragments and silicon-containing species from the substrate polymer layer. PC 2 (Figure 8b) reflects the image features that correspond to the salt ions, including Cl^- , NaOH^- , CaO^- , etc., (bright regions) and SDS fragments (dark regions). PC 3 (Figure 8c) captures the image feature that corresponds to the halo around the probe spot (dark regions). The PC 3 loadings plot (Figure 8c) indicates that most major peaks with negative PC 3 loadings associated with the halo in the TOF-SIMS image are silicon- and sulfur-containing fragments possibly from the polymer-coated glass substrate exposed as a result of polymer layer damage from the microarray printing process (for more details see Figures S4 and S5, Supporting Information) or from silicon-containing contaminants wicking to the outside of the spot upon spotting. Capillary phenomena during drying have been suggested as the reason for the appearance of ringlike halo features in other contexts (e.g.,

drying of nanoparticle solutions).^{41,42} Other factors such as surface tension, droplet shape, and droplet impact on the substrate could also play a role. Further study is required to address this issue in further detail.

Conclusions

Imaging XPS and imaging TOF-SIMS are complementary, sensitive tools for analysis of elemental composition, chemical structure, relative density, and spatial distributions of micropatterned DNA arrays on glass substrates. Combined with routine fluorescence imaging, a more complete assessment of the chemistry and physical disposition of DNA array spotting can be realized. Individual DNA microarray spots were analyzed at high resolution for the first time. A combination of XPS imaging and small spot analysis allowed identification of the micropatterned DNA arrays and quantification of DNA elements within individual microarray spots to determine probe immobilization and hybridization efficiencies. XPS comparisons of DNA immobilized in both macrospot and microarray formats demonstrated distinct differences in probe densities and hybridization efficiencies resulting from the two different printing processes (nonequilibrium drying microarray printing process vs macrospot reactions). Imaging TOF-SIMS provided different information on DNA spatial distribution and relative density, even against a complex organic matrix background. Bromine modification of the DNA bases provides unique target DNA fragments in TOF-SIMS data and high quality images of DNA microspots with little interference from the other organic species present in the surface region. Finally, application of PCA to

TOF-SIMS imaging datasets provided new, unique information not readily observable in the univariate TOF-SIMS images alone, allowing identification of species involved in spot nonuniformities (e.g., “halo” often observed in fluorescence images). The ability to accurately quantify surface-immobilized DNA molecules with these methods is more convenient than radiolabeling and more informative than fluorescence scanning alone. The approach is likely to prove extremely useful in the future development and optimization of micropatterned DNA surfaces to improve the performance and accuracy of genomic arrays and biosensor applications. Obtaining detailed information about distribution of chemical species within a DNA microspot is the first step in developing correlations between the DNA surface properties (i.e., structure and composition) and hybridization properties at the microscopic level. This information is also needed to determine the influence of experimental conditions (print additives, nonequilibrium drying, buffer, etc.) on the DNA surface structure and composition.

Acknowledgment. The authors gratefully acknowledge support from NESAC/BIO (NIH Grant No. EB-002027) and NIH Grant EB-001473. Dan Graham is thanked for assistance with PCA analysis. We also thank Steve Golledge for expert technical assistance with the TOF-SIMS experiments performed at the Center for Advanced Materials Characterization in Oregon. Ping Gong is thanked for her technical assistance and for supplying patterned arrays used for exploratory XPS imaging experiments done prior to experiments reported in this study.

Supporting Information Available: Experimental data are available as Supporting Information. This material is available free of charge via the Internet at <http://pubs.acs.org>.

JA071879M

(41) Maillard, M.; Motte, L.; Ngo, A. T.; Pileni, M. P. *J. Phys. Chem. B* **2000**, *104*, 11871–11877.

(42) Ohara, P. C.; Heath, J. R.; Gelbart, W. M. *Angew. Chem., Int. Ed. Engl.* **1997**, *36*, 1078–1080.